ELSEVIER

Journal of Photochemistry and Photobiology A: Chemistry 102 (1996) 13–20

Journal of PHOTOCHEMISTRY AND PHOTOBIOLOGY A:CHEMISTRY

Photodissociation dynamics of iodobenzene by state-selective photofragment translational spectroscopy

Hyun Jin Hwang [a], Mostafa A. El-Sayed [b]

[a] *Department of Chemistry, Kyung Hee University, Seoul 130-701, South Korea*

[b] *School of Chemistry and Biochemistry, Georgia Institute of Technology, Atlanta, GA 30332-0400, USA*

Abstract

State-selective photofragment translational spectroscopy is used to probe the detailed nature of the photodissociation dynamics of iodobenzene at 304 nm. Simultaneous determination of the recoil speed, the spatial anisotropy, and the final state of the iodine fragment reveals that three dissociation channels with different dynamical characteristics compete in the photodissociation of iodobenzene at 304 nm. Based on the observed energy partitioning between the internal and translational modes and the dissociation time t_d determined from the spatial anisotropy by using a rotational depolarization model, the three dissociation channels are assigned as follows. Two fast dissociation channels, which result in formation of $I^*(^2P_{1/2})$ ($t_d = 0.4$ ps, quantum yield $\Phi = 0.005 \pm 0.002$) and high velocity $I(^2P_{3/2})$ ($t_d = 0.3$ ps, $\Phi = 0.70 \pm 0.04$), are due to a parallel transition to the repulsive $^3Q_0(n,\sigma^*)$ state in the C–I bond, followed by dissociation along the same state or curve crossing to the $^1Q_1$ state respectively. A slow dissociation channel ($t_d = 0.5 - 1.4$ ps, $\Phi = 0.30 \pm 0.04$) which produces low velocity $I(^2P_{3/2})$ is due to a parallel transition to the triplet π,π^* state(s) in the phenyl ring that is predissociated by the repulsive n,σ^* state(s). The dissociation times determined in the present work are in excellent agreement with those of the recent femtosecond real-time measurements by Cheng et al. at 278 nm (P.Y. Cheng, D. Zhong and A.H. Zewail, *Chem. Phys. Lett., 237* (1995) 399).

Keywords: Photodissociation; Dynamics; Iodobenzene; Photofragment translation spectroscopy

1. Introduction

Since Wilson and coworkers [1] introduced the time-of-flight (TOF) photofragment translational spectroscopy method, much attention has been paid to the translational properties of photofragments, which in turn provide detailed knowledge for the photodissociation dynamics of isolated molecules (for reviews see, for example, Ref. [2]). Measurements of photofragment recoil speed distributions allow one to determine internal energy distributions of photofragments [2] (and often vibrational [3–5] or rotational [6] state distributions with sufficiently high resolution) via energy conservation. This is of much value especially for polyatomic fragments that cannot be probed directly by state-specific optical methods such as laser-induced fluorescence and resonance-enhanced multiphoton ionization (REMPI). Another important measurable quantity is the angular distribution of the photofragment with respect to the electric vector of the photolysis light. Knowledge of this property allows the symmetry of the excited state as well as the time scale of photodissociation to be inferred [2,7–10].

Several variations of the TOF method have been developed recently by employing a simple TOF mass spectrometer and a state-selective detection scheme using REMPI [11–15]. In these "state-selective TOF photofragment translational spectroscopy" techniques, photofragments are ionized immediately after photodissociation by REMPI and allowed to drift in a field-free condition (or in the presence of a weak electric field) before being accelerated toward the detector to bring about velocity resolution in the arrival time. While the low resolution of this type of method makes it difficult to determine accurately the translational properties of photofragments, their state selectivity to probe individual quantum states gives advantages in measuring various correlations between different photofragment properties such as the recoil speed, the recoil direction, the quantum state, and the rotation vector of a photofragment. Several groups [15,16] have recently examined such correlations and have been able to extract more detailed information on the nature of the photodissociation dynamics.

Recently, we have employed one form of state-selective photofragment translational spectroscopy which utilizes a time-delayed pulsed-acceleration TOF mass spectrometer[17]. We have improved the velocity resolution of the technique by employing a small discrimination aperture in front of the detector to reduce the detection solid angle. This

PII S1010-6030(96)04369-9

modification also makes it possible to determine photofragment recoil speed and angular distributions through direct deconvolution of TOF distributions [18]. This method has been used to study photodissociation of various iodide molecules [17–23].

In this work, we investigate the photodissociation dynamics of iodobenzene at 304 nm through simultaneous determination of the recoil speed distribution, the spatial anisotropy, and the quantum state of the iodine atom fragment in either the ground I($^2P_{3/2}$) or the spin-orbit excited I*($^2P_{1/2}$) state (hereafter denoted by I and I* respectively). This correlated measurement of three properties allows us to differentiate unambiguously multiple dynamical channels in the complex photodissociation reaction of iodobenzene. While the recoil speed distribution is used to monitor the energy partitioning between the translational and internal modes of the photofragments, the spatial anisotropy is used to determine the dissociation time by means of a rotational depolarization model.

As reported in our previous communication [21], UV photodissociation of iodobenzene can take place via two different types of dissociation processes with different dynamical characteristics. This is due to the presence of the π,π^* electronic system in the phenyl ring in addition to the n,σ^* electronic system in the C–I bond. It is well known for alkyl iodides [24–29] that three excited states arising from the n,σ^* transition, $^3Q_1$, $^3Q_0$, and $^1Q_1$ in order of increasing energy, are repulsive, resulting in prompt dissociation along the C–I bond. This type of dissociation must lead to formation of photofragments with high translational energy and high spatial anisotropy as in alkyl iodides. In contrast to the n,σ^* states, the π,π^* states of aromatic iodides are bound with respect to the dissociation coordinate at the zeroth-order level of description. Bersohn and coworkers [10,30] have observed that photodissociation of aryl halides at the photon energies within the singlet π,π^* states results in high internal excitation of the aromatic fragment with reduced spatial anisotropy. These observations were interpreted as due to excitation of the singlet π,π^* state(s) followed by predissociation via the repulsive n,σ^* state(s). Thus, if any benzene-type state is excited in iodobenzene at 304 nm (below the excitation energy of the first singlet π,π^* state), this will lead to a slower dissociation that results in reduction in the spatial anisotropy and increase in the internal excitation of the phenyl ring compared with the photodissociation of alkyl iodides.

Consistent with the simple expectation described above, the two different types of dissociation processes are found to compete in the photodissociation of iodobenzene at 304 nm. In both I and I* formation channels, dissociation processes similar to those of the alkyl iodide have been observed that represent high recoil speeds with narrow distributions and high parallel-type anisotropy. These two channels can be attributed to the alkyl iodide type fast dissociation resulting from the n,σ^* transition. An additional dissociation process, that can be attributed to a slow dissociation due to excitation of the lowest triplet π,π^* state(s), has been observed in the I formation channel which represents a broad slow recoil speed distribution with a broad range of parallel-type anisotropy.

Details of the evidence and discussions are presented for the mechanism and dynamics of the dissociation channels summarized above. In addition an interesting issue is addressed for the dissociation times of the different channels. Recently, Cheng et al. [31] performed femtosecond real-time experiments at 278 nm and directly determined the dissociation times of the two recoil velocity components of the I fragment. Comparison of their results with the results obtained in this work from the rotational depolarization analysis gives excellent agreement.

2. Experimental details

Details of the experimental apparatus and methodology have been described previously [17,18]. Briefly, a single-stage pulsed-acceleration TOF mass spectrometer was used in combination with a linearly polarized nanosecond-pulsed laser to measure the recoil velocity distribution of state-selected iodine atom photofragments produced from photodissociation of iodobenzene at 304 nm. Neat vapor of iodobenzene at room temperature (about 0.2 Torr) was introduced effusively into the ionization region of the TOF mass spectrometer (about 1×10^{-6} Torr) via approximately 1 mm diameter Teflon tubing. A linearly polarized, focused laser pulse with ca. 6 ns pulse width was used to dissociate iodobenzene molecules and also to ionize state selectively the resulting iodine atom photofragments within the same laser pulse via 2+1 REMPI. Experiments were performed at two wavelengths, 304.67 nm and 304.02 nm (ca. 30 μJ pulse^{-1}, the doubled output of a pulsed dye laser pumped by the 532 nm second harmonic of a Q-switched Nd:YAG laser), to ionize selectively the ground and spin–orbit excited iodine atoms respectively. The angular and the recoil speed distributions of the photodissociated iodine atoms in each selected state were determined by measuring the TOF distributions of the iodine ions at two laser polarization angles $\alpha=0°$ and 90°, with respect to the detection axis.

Following photodissociation and photoionization, the ions produced are allowed to recoil under a field-free condition according to their recoil velocities imparted from photodissociation. After a delay time of 1.5 μs, an acceleration electric field of ca. 1010 V cm^{-1} is pulsed for 1.0 μs and the TOF distribution of the iodine ions are measured after travel through a 78 cm field-free drift. Because of this time-delayed pulsed acceleration, the TOF measured in the present method depends on the component of the photofragment recoil velocity along the detection axis [17,18]. In addition, a discrimination aperture with a 6.0 mm diameter is mounted in front of the MCP detector to reduce the detection solid angle and thus to detect only those ions whose recoil directions are aligned close to the detection axis. This greatly enhances the

velocity resolution of the method and facilitates the deconvolution procedure to determine separately the recoil speed and spatial distributions from the measured TOF distributions [17,18].

Iodobenzene was purchased from Aldrich and used after distillation at about 8 Torr and about 58 °C. In order to check impurities, electron impact ionization mass spectra were taken in a magnetic sector mass spectrometer. Before distillation, very small amounts of diiodobenzene and I_2 were found in the mass spectrum, but no mass signals from diiodobenzene were observed and the I_2 mass peak was greatly reduced after distillation. TOF spectra were examined in our apparatus for both distilled and undistilled samples but no difference was found, suggesting that our results are free from contamination. TOF spectra presented in this paper display small peaks due to I_2 that was purposely added for calibration of apparatus constants as described previously [17,18]. Photodissociation of I_2 at the wavelengths used is well characterized [19] and does not produce iodine atoms which overlap with those from iodobenzene in their velocities.

3. Results and analysis

3.1. Recoil velocity distribution

TOF distributions h^{α}(TOF) of iodine ions measured at two laser polarization angles $\alpha = 0°$ and 90° with respect to the detection axis were used to determine the recoil velocity distribution $f(v,\theta)$ of the state-selected iodine fragment, where v and θ denote the recoil speed and the recoil angle with respect to the electric vector of the photolysis light respectively. Details of this transformation method are described elsewhere [18]. The expression for $f(v,\theta)$ is taken to be

$$f(v,\theta) = \frac{1}{4\pi}[1 + \beta(v)\, P_2(\cos\theta)]\, g(v) \qquad (1)$$

where $P_2(\cos\theta) = (3\cos^2\theta - 1)/2$ is the second-order Legendre polynomial. $g(v)$ and $\beta(v)$ are the recoil speed distribution and the anisotropy parameter respectively. Note that we express the anisotropy parameter as a function of v. This form is more general (compared with taking it as a constant parameter that is valid only for prompt photodissociation) in representing various types of photodissociation processes such as the case involving more than one transition with different polarizations or a wide range of dissociation times as in the present case. The value of β must lie in the range $-1 \le \beta \le 2$. The two limiting values -1 and 2 correspond to the case of prompt photodissociation with the transition dipole moment lying perpendicular and parallel to the dissociation bond axis respectively.

Fig. 1 shows TOF distributions of resonantly ionized I atoms produced from the photodissociation of iodobenzene at 304.67 nm (25 μJ pulse^{-1}) at $\alpha = 0°$ and 90°. Shown in Fig. 2(a) are the recoil speed distribution $g(v)$ and the anisotropy parameter $\beta(v)$ of I at 304.67 nm. These are obtained from the TOF distributions shown in Fig. 1. It is clear in Fig. 2(a) that the I atoms are produced with two different recoil velocity distributions, a sharp distribution at the high recoil speed with a very high parallel anisotropy and a broad distribution at the lower recoil speed with a lower parallel anisotropy. In order to examine the two distributions separately, we have decomposed the recoil velocity distribution of the I atom into two components as shown in Fig. 2(b). In this decomposition procedure, we have extracted the high recoil velocity distribution by assuming that its characteristics, the shape of $g_h(v)$ and the recoil speed dependence of $\beta_h(v)$, are analogous to those of the I* formation channel of C_2F_5I (Fig. 3), a representative case [17] of a direct dissociation

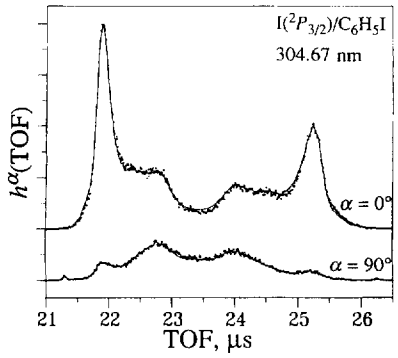

Fig. 1. TOF distributions h^{α}(TOF) of resonantly ionized I atoms produced from photodissociation of iodobenzene at 304.67 nm at two laser polarization angles $\alpha = 0°$ and 90° with respect to the detection axis: ·, experimental results; ———, results obtained by back transforming $g(v)$ and $\beta(v)$ shown in Fig. 2(a). The small peaks observed at TOF values of about 21.3 and 26.2 μs at $\alpha = 90°$ are due to photodissociation of I_2 which was purposely introduced for calibration of instrumental parameters.

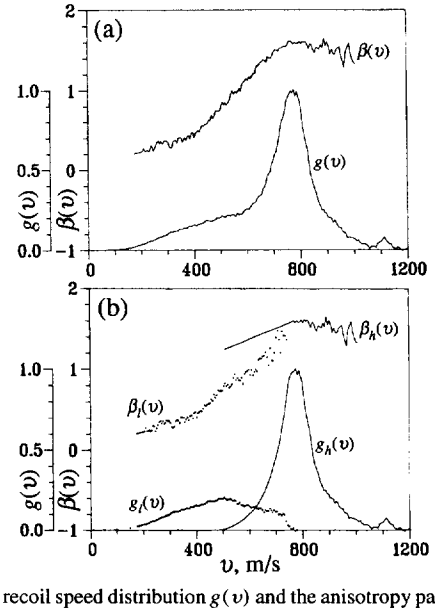

Fig. 2. The recoil speed distribution $g(v)$ and the anisotropy parameter $\beta(v)$ of I atoms produced from photodissociation of (a) iodobenzene at 304.67 nm and (b) its two recoil velocity components. These are obtained from the TOF distributions shown in Fig. 1 by using the transformation method described in Ref. [18]. The small peak observed at $v = 1110$ ms^{-1} is due to photodissociation of I_2 that was introduced for calibration purpose.

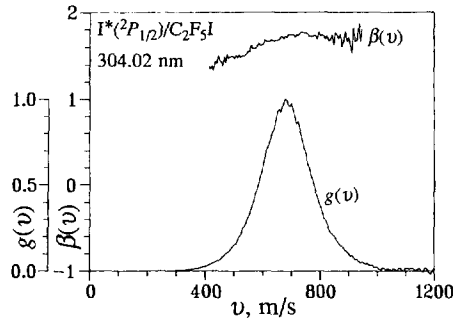

Fig. 3. The recoil speed distribution $g(v)$ and the anisotropy parameter $\beta(v)$ of I* atoms produced from photodissociation of C_2F_5I at 304.02 nm.

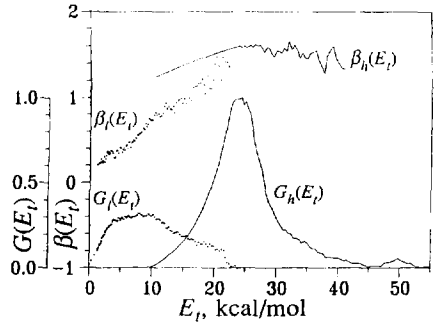

Fig. 4. The same as Fig. 2(b) but as a function of translational energy release E_t. The representative values of the energetics and the anisotropy parameter for the two distributions are summarized in Table 1.

resulting from a pure parallel transition. This assumption is based on the observed similarities between these two photodissociation processes, i.e. both cases exhibit very sharp, high recoil speed distributions with high parallel anisotropy values that are independent of the recoil speed. In order to examine the photofragment distribution as a function of translational energy release E_t (i.e. translational energy of both photofragments), $g(v)$ and $\beta(v)$ shown in Fig. 2(b) are transformed into the energy domain $G(E_t)$ and $\beta(E_t)$ according to the momentum conservation rule. The results are shown in Fig. 4. The average translational release $\langle E_t \rangle$ and full width at half-maximum (FWHM) of $G(E_t)$ are summarized in Table 1.

Fig. 5 shows TOF distributions and corresponding $G(E_t)$ and $\beta(E_t)$ for state-selectively ionized I* atoms produced at 304.02 nm (25 μJ pulse^{-1}). In contrast to the I channel, the translational energy release distribution $G(E_t)$ of the I* channel represents a single relatively sharp distribution. The observed trend of β is similar to that of the high translational energy distribution of the I channel shown in Fig. 4 and also that of the I* formation channel of C_2F_5I shown in Fig. 3, suggesting that the center-of-mass value of β is independent of v for this channel. The value of β is observed to be high and independent of v on the high energy side while it is decreasing on the low energy side as E_t does. Similar to the I* channel of C_2F_5I (see Fig. 3), the decrease in β on the low energy side can be understood in terms of the broadening effect due to the parent molecule velocity.

As will be discussed in detail in Section 4.2, the observed differences in recoil speed distributions and the recoil speed dependence of β can best be attributed to the different dynamics involved in the three dissociation channels. While the I* and the high velocity I channel can be attributed to very fast dissociation resulting from a parallel transition to the repulsive n,σ^* state in the C–I bond, the low velocity I channel can be attributed to slow dissociation due to a parallel transition to the bound π,π^* state in the phenyl ring which is predissociated by the repulsive n,σ^* state.

3.2. Energy partitioning and quantum yields

During the photodissociation, total energy is conserved and thus excess energy over the dissociation energy is partitioned into the translational and internal modes of two fragments [4]. The available energies E_{avl} and E^*_{avl} for the I and I* channels respectively are related to the translational energy release E_t and the internal energy E_{int} of the phenyl radical as follows:

$$E_{avl} = h\upsilon - D^0_0 + E^p_{int} = E_t + E_{int} \quad (2)$$

$$E^*_{avl} = E_{avl} - E_{so} = E^*_t + E^*_{int} \quad (3)$$

where D^o_o is the dissociation energy of the ground state iodobenzene into the ground state phenyl radical and iodine atom at 0 K, E^p_{int} is the internal energy of the parent molecule (2.8 kcal mol^{-1} on the average at room temperature), and E_{so} is the spin-orbit excitation energy of the iodine atom (21.7 kcal mol^{-1}). D^o_o can be estimated from the value of the dissociation energy at room temperature D^o_{298} (65.4 ± 2 kcal mol^{-1} [32]) by making a thermal correction of 1.5 kcal mol^{-1} (The thermal correction for the dissociation energy can be estimated by considering changes in molar enthalpies of the chemical species involved in the photodissociation reaction $C_6H_5I \rightarrow C_6H_5 + I$. At room temperature, C_6H_5I, C_6H_5, and I have molar enthalpies (relative to those at 0 K) of $4RT$, $4RT$, and $5/2RT$ respectively due to translation, rotation, and the

Table 1
Summary of photodissociation dynamics of iodobenzene at 304 nm [a]

Iodine state	λ (nm)	Quantum yield	$\langle E_{avl} \rangle$	$\langle E_t \rangle$	FWHM of $G(E_t)$	$\langle E_{int} \rangle$	$\langle E_t \rangle / \langle E_{avl} \rangle$	β	t (ps)
I*	304.02	0.005 ± 0.002	11.2	9.2 ± 0.2	5.7 ± 0.2	2.0	0.82	1.5 ± 0.1	0.42
I	304.67	0.70 ± 0.04	32.7	24.8 ± 0.2	8.3 ± 0.2	7.9	0.76	1.60 ± 0.05	0.34
	304.67	0.30 ± 0.04	32.7	10.2 ± 0.4	15.0 ± 0.6	22.5	0.31	1.4 − 0.2	0.5 − 1.3

[a] Energies are in kilocalories per mole. Uncertainties shown are one standard deviation of 3 or 4 measurements. The dissociation times t_d are determined from the measured values of the anisotropy parameter β using the time-anisotropy correlation shown in Fig. 6. See text for details.

pressure-volume term PV, if all the species are considered to be ideal gases. Vibrational energies of C_6H_5I and C_6H_5 at roomtemperature would be similar considering the similar numbers of the vibrational modes, and thus their difference could be ignored. Therefore, the enthalpy change D°_{298}, of the reaction is expected to be greater than that D°_0 at 0 K, approximately by $5/2RT = 1.5$ kcal mol^{-1}. See Ref. [33]). Values for the energy partitioning calculated by using this value of D°_0 (63.9 ± 2 kcal mol^{-1}) are listed in Table 1.

We have determined the quantum yield of $\Phi(I^*)$ of I* from the relative ion signal s_I^*/s_I observed for the I* and I atoms produced at 304.02 nm and 304.67 nm respectively. Assuming that absorption strengths at these two wavelengths are the same, one can write the following equations:

$$\Phi(I^*) = \frac{n_I^*/n_I}{n_I^*/n_I + 1} \tag{4}$$

and

$$\frac{s_I^*}{s_I} = \frac{n_I^* f_I^*}{n_I f_I} \tag{5}$$

As shown in Eq. (5), the number ratio n_I^*/n_I of the iodine atoms produced in the two states can be determined from the relative ion signal s_I^*/s_I at the same photon flux, if the relative ionization efficiency f_I^*/f_I is known. The relative ion signal is determined to be 0.007 ± 0.001. The relative ionization efficiency is determined by studying the photodissociation of I_2 at the same wavelengths and also at the same laser pulse energy to avoid a possible photon flux dependence. At these wavelengths, I_2 is known [19] to dissociate into $I + I^*$, i.e. n_I^*/n_I, is equal to 1 and thus $f_I^*/f_I = s_I^*/s_I$ for I_2. The value of f_I^*/f_I is measured to be 1.3 ± 0.2. Using this value, we obtain the quantum yield of I* at about 304 nm to be 0.005 ± 0.002. This value agrees well with the upper limit value estimated by Pence et al. [34] at 308 nm (0.004). The quantum yields of the low and high velocity components of I are thus determined to be 0.30 ± 0.04 and 0.70 ± 0.04 respectively.

3.3. Time dependence of anisotropy parameter

The anisotropy parameter β can be related to the dissociation time via rotational depolarization. Many researchers [7–10] have treated this time-anisotropy correlation assuming a purely rotational depolarization. We use the results of Yang and Bersohn [9] for the symmetric top molecule to relate the observed β to the dissociation time t_d, since the moments of inertia around the axes perpendicular to the figure axis are almost equal in iodobenzene [10]. In this model, the anisotropy parameter $\beta(t)$ observed at time t is related to the initial value β_o at time zero [9]:

$$\beta(t) = \beta_o \langle D^2_{o,o}(t) \rangle \tag{6}$$

where $\langle D^2_{o,o}(t) \rangle$ is the rotational correlation function and the brackets denote the average over the rotational ensemble. The

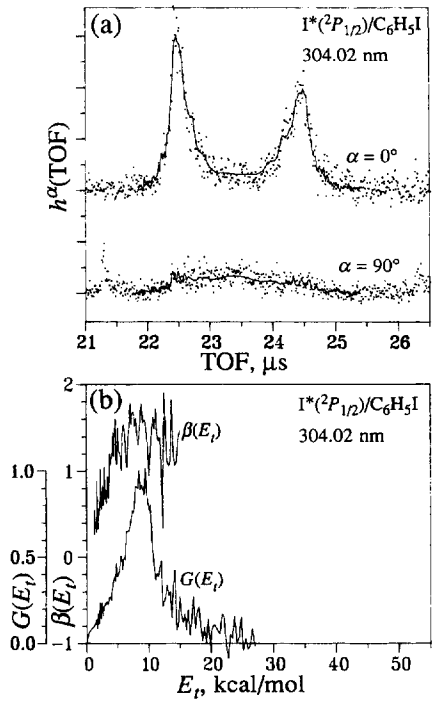

Fig. 5. (a) TOF distributions h^α(TOF) of resonantly ionized I* atoms produced from photodissociation of iodobenzene at 304.02 nm(●, experimental results; —, results obtained by back transforming $G(E_t)$ and $\beta(E_t)$ shown in (b)) and (b) corresponding $G(E_t)$ and $\beta(E_t)$.

rotational correlation function depends on the temperature T and the asymmetry parameter $b = (I - I_z)/I_z$, where I_z is the moment of inertia around the figure axis and I is that around an axis perpendicular to the figure axis. The time dependence of the rotational correlation function calculated for room temperature iodobenzene ($b = 7.05$) is shown in Fig. 6.

In the original treatment of Yang and Bersohn [9], the rotational correlation function was averaged, in addition to the rotational averaging, over a range of dissociation times assuming that the dissociation probability follows a first-order kinetics with a dissociation lifetime τ_d. However, we exclude this averaging. Our results show that the value of β in the low velocity I channel is dependent on the recoil velocity, implying that the dissociation events taking place at dif-

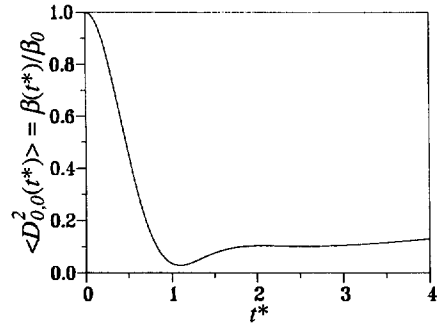

Fig. 6. The rotational correlation function relevant to the photodissociation of iodobenzene. t^* is the reduced dissociation time defined as $t^* = t\ (I/kT)^{-1/2}$, where I is the moment of inertia around an axis perpendicular to the figure axis of the symmetric top molecule, k is the Boltzmann constant, and T is the temperature of the parent molecule. For room temperature iodobenzene, $(I/kT)^{1/2}$ is equal to 1.70 ps.

ferent dissociation time result in different values of β. Therefore, the value of β observed at each value of v (or E_t) must be related to each dissociation time t_d rather than the dissociation lifetime τ_d which represents an averaged dissociation time within the assumed kinetics and is related to an average value of β as in the treatment of Yang and Bersohn [9].

If the vibrational motion can be ignored, β_o in Eq. (6) is given by [7–9]

$$\beta_o = 2P_2(\cos\chi) \tag{7}$$

where χ is the angle between the transition dipole moment of the parent molecule and the dissociation bond axis. To include the effect of vibrational motion, one can take an average over a vibrational ensemble in Eq. (7) because the vibrational and rotational motions are well separated in time. Alternatively, we rewrite Eq. (7) as follows:

$$\beta_o = 2\kappa P_2(\cos\chi) \text{ with } \kappa \leq 1 \tag{8}$$

where the parameter κ takes into account the effect of the vibrational motion and also the decrease in β due to the thermal distribution of the parent molecule velocity. In general, the parameter κ depends on the dissociation time and the recoil speed. The fact that the values of β observed for the I* channel and the high velocity I channel (about 1.5 and about 1.6 near the peak respectively; see Figs. 4 and 5) are very close suggests that the recoil speed dependence of κ due to the parent molecule velocity is rather weak. Therefore, we expect that Eq. (8) with a constant value of κ will be valid for a given molecule when the dissociation time is longer than the vibration period, thus allowing effective averaging over the vibrational motion. The lower limit of κ can be estimated as follows. The value of β observed for the I* channel of C_2F_5I (about 1.75) shown in Fig. 3 is the highest value for the parallel transition (i.e. $\chi = 0°$) among various iodide molecules studied with our method. According to Eqs. (6) and (8), this value should be equal to β_o $\langle D^2_{o,o}(t)\rangle = 2\kappa\langle D^2_{o,o}(t)\rangle \leq 2\kappa$. Thus, we find the lower limit of κ to be about 0.88.

From the time dependence of the rotational correlation function shown in Fig. 6, the dissociation times for the three observed dissociation processes can be determined. The high parallel anisotropy parameters observed for the I* channel (about 1.5) and the high velocity I channel (about 1.6) suggest that the transition dipole moments are aligned parallel to the C–I bond for these channels. Taking $\chi = 0°$ and $\kappa = 0.9$, we obtain the dissociation time of 0.4 ps for the I* channel and 0.3 ps for the high velocity I channel. Uncertainties involved in determining the dissociation time are expected to be rather small (within 0.1 ps). For example, taking $\kappa = 1$ (i.e. ignoring the effects of the vibrational motion and the parent molecule velocity), one obtains dissociation times that are only 0.1 ps longer than those when $\kappa = 0.9$.

The value of β observed in the low velocity I channel (see Fig. 4) exhibits a strong translational energy dependence. As discussed in detail in Section 4, this must be interpreted as due to a slow dissociation with a broad range of dissociation time. Through the correlation between the dissociation time and β shown in Fig. 6, the time dependence of E_t is obtained and shown in Fig. 7. In this analysis, we assumed that the corresponding transition is a purely parallel type (i.e. $\chi = 0°$ and $\beta_o = 2\kappa$) and the value of κ is equal to 0.9 to include the effects of the vibrational motion and the parent molecule velocity. As shown in Fig. 7, the dissociation time is relatively long and has a broad range (0.5 – 1.4 ps) compared with the rotation period of the parent molecule (1.70 ps). The observed dependence is approximately linear with a slope $dE_t/dt \approx -23$ kcal mol^{-1} ps^{-1}.

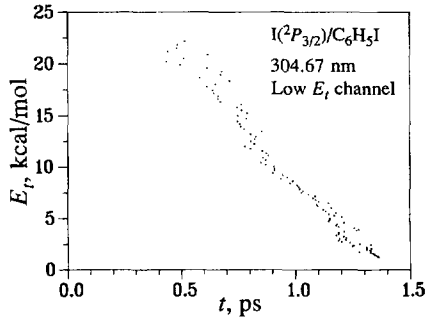

Fig. 7. Dissociation time dependence of translational energy release E_t determined for the low recoil velocity distribution of the I channel. This dependence was obtained by comparing the E_t dependence of β shown in Fig. 4 and the time-anisotropy correlation shown in Fig. 6. The observed time dependence of E_t is approximately linear with a slope of -23 kcal mol^{-1} ps^{-1}.

4. Discussion

4.1. Dissociation time and rotational depolarization

As presented in Section 3.3, the rotational depolarization model of Yang and Bersohn [9] was used to determine the dissociation times of the three dissociation channels of iodobenzene at 304 nm from the observed values of β. By assigning the three dissociation channels to transitions polarized parallel to the C–I bond, we obtain the dissociation times for the I*, high velocity I, and low velocity I channels to be 0.4 ps, 0.3 ps, and 0.5 – 1.4 ps respectively. While single values are obtained for the I* and high velocity I channels from the constant values of β, a broad range of dissociation times is obtained for the low velocity I channel from the observed range of β which is dependent on E_t. These results are in excellent agreement with the recent results of the femtosecond real-time pump–probe experiments at 278 nm by Cheng et al. [31], supporting our rotational depolarization picture. They observed that the high velocity I transient rises as fast as their instrumental response (i.e. with zero rise time) but with a time delay of 400 fs. This observation is in excellent agreement with our result for this channel. In the low velocity I channel, they observed a slow build-up with a single-exponential rise time of 550 fs. By taking the time range for the 550 fs rise time build up from 5% to 95% of the total intensity

and adding the time delay of 400 fs observed for the high velocity I channel, the range of dissociation time for this channel is estimated to be from 0.4 to 2.0 ps. This is also in excellent agreement with our result.

As discussed above, the agreements between the two experiments are surprisingly good, suggesting that our rotational depolarization picture with the assignments of the three channels to parallel transitions is valid. The I* and high velocity I channels dissociate promptly with single values of the dissociation time, thus resulting in constant values of β. The low velocity I channel dissociates slowly with a broad range of dissociation times, giving rise to a range of values of β. As discussed by us previously [21], the E_t dependence of β in this channel implies that the intramolecular vibrational energy transfer toward the phenyl ring modes takes place in time, thus resulting in more energy partitioning toward the phenyl ring vibration modes (i.e. less to the translation mode) at the longer dissociation time as observed. This suggests that the slope of the near-linear time dependence of E_t ($dE_t/dt \approx -23$ kcal mol^{-1} ps^{-1}; see Fig. 7) can be attributed to the rate of IVR as proposed previously [21].

It is interesting to point out that there is a subtle difference in the two methods in probing the dissociation time. While our method probes a time lapse of the dissociation event from the Frank–Condon region to an internuclear distance where the rotational depolarization is ineffective, the real-time pump-probe method measures a time lapse needed to reach an internuclear separation where the photofragments are spectroscopically free from each other. The excellent agreements observed for the two experiments suggest that the two methods in fact probe a similar final internuclear distance in the potential energy surface.

4.2. Properties of electronic states at 304 nm excitation

As summarized in Table 1, two types of dissociation, leading to three reaction channels, are found to compete in the photodissociation of iodobenzene at 304 nm. The I* channel and the high velocity I channel can be attributed to alkyl iodide type direct dissociation resulting from excitation to the repulsive n,σ^* state in the C–I bond. The highly repulsive nature of the excited states involved in these two channels is manifested by the high degree of energy partitioning toward translation as well as the high degree of anisotropy. The observed values of $\langle E_t\rangle/\langle E_{avl}\rangle$ and FWHM of $G(E_t)$ (see Table 1) are between the values observed for CF_3I [22] and C_2F_5I [17] at the same photolysis wavelength, indicating that the excited states involved are the repulsive n,σ^* states as in alkyl iodides [24–29]. The highly anisotropic values of β (and thus the short dissociation times) observed in these two channels also support this conclusion. Based on the photodissociation mechanism of alkyl iodides [24–29], the I* channel and the high velocity I channel can be attributed to the parallel transition to the $^3Q_0$ state followed by dissociation along the same state to produce I* or curve crossing to the $^1Q_1$ state to produce I.

In gross view of our results, the n,σ^* states of iodobenzene seem to be well localized in the C–I bond despite the presence of the π,π^* states in the phenyl ring. There are, however, some evidences for interactions between the n,σ^* and π,π^* electronic systems. First, the curve-crossing probability from the $^3Q_0$ to the $^1Q_1$ state is strongly enhanced (99%) compared with alkyl iodides. This large enhancement is a result of a strong coupling between the $^3Q_0$ and $^1Q_1$ states induced by interaction with the more polarizable phenyl ring. Second, the values of β for the I* (1.5) and the high velocity I (1.6) are slightly reduced compared with those observed for the I* channels of CF_3I and C_2F_5I (about 1.75 at the peak velocity). This indicates that the n,σ^* states of iodobenzene dissociate in a slightly longer time scale than those of alkyl iodides within the picture of the rotational depolarization model. Because of interaction with the π,π^* states of the phenyl ring, the n,σ^* states in iodobenzene become less repulsive and thus result in slower dissociation compared with alkyl iodides. The femtosecond real-time measurement of Cheng et al. [31] is also consistent with this conclusion. In their experiment, the high velocity I channel at 278 nm is observed with a dissociation time of 400 fs, which is ca. 200 fs longer than that of ICN [35] at the similar recoil velocity.

The presence of an additional low velocity I channel in iodobenzene must then be attributed to excitation of the benzene-type π,π^* excited state(s) which is predissociated by non-radiative mixing with the nearby n,σ^* states dissociating into I. This mixed benzene-type excited state(s) must result in a longer dissociation time than those of the pure n,σ^* states as observed. This, as well as the larger number of internal degrees of freedom in the phenyl ring, allows for efficient energy redistribution, resulting in a broader translational energy distribution with a lower average translational energy than that produced from dissociation from the repulsive n,σ^* state (see Table 1).

Since the first excited π,π^* state of iodobenzene is located way above the photon energy used [36] and the observed low parallel-type anisotropy (0.72 on the average with a broad range from 0.2 to 1.4) can be explained by the rotational depolarization of a pure parallel transition as discussed in Section 4.1, the low velocity I channel must result from a parallel transition to the triplet π,π^* state(s). In benzene, the excitation energy of the first triplet π,π^* state is lower than the photon energy but that of the second triplet is ca. 3600 cm^{-1} higher. The excitation energies of these triplet states will certainly be lowered in iodobenzene by mixing with the charge-transfer-type states of iodobenzene, but no calculations are available. Therefore, we consider the two lowest triplet π,π^* states as possible candidates. The lowest triplet state of iodobenzene is the ^3L_a state which is of $^3A_1$ symmetry. The second triplet state is the ^3L_b state of $^3B_2$ symmetry. Absorption (or emission) of the $^3A_1$ and $^3B_2$ states of iodobenzene polarized in the benzene plane can be predicted by use of spin–orbit vibronic coupling perturbations, as was done to explain the phosphorescence polarization properties of haloaromatic molecules [37]. Note that in this type of

perturbation treatment the polarization characteristic of absorption is determined by the symmetry of the perturbing state from which the zeroth-order state borrows absorption strength [37]. This suggests that the perturbing state must be the strongly radiative $^1A_1$ state(s) that is polarized in the benzene plane along the C–I bond. It is interesting to note that the transition from the ground covalent state to the strongly radiative charge-transfer-type ionic state (a $^1A_1$ state) in iodobenzene is a good radiative source for the triplet states of iodobenzene [38]. This could make the vibronically induced spectrum dominantly parallel to the C–I bond.

5. Conclusion

By the use of a photofragment translational spectroscopy technique, we were able to differentiate different photodissociation channels of iodobenzene at 304 nm. Not only can the energy partitioning between the internal and translational modes be determined directly but also the time scale of the photodissociation can be obtained from the observed values of β. This makes it possible to identify unambiguously the complex photodissociation mechanism of iodobenzene which involves two different types of the excited states, i.e. the alkyl iodide type repulsive n,σ^* states and the benzene-type predissociative triplet π,π^* states. It is noteworthy that the dissociation times determined by the rotational depolarization model in the present work are in excellent agreements with the femtosecond real-time pump-probe measurements of Cheng et al. [31]. This demonstrates that photofragment translational spectroscopy is a powerful technique to determine the dissociation time scale which is comparable with or shorter than the molecular rotation period.

Acknowledgements

The authors wish to thank the National Science Foundation for its support of this work. H.J.H. acknowledges the Ministry of Education, Korea, and the Korea Science and Engineering Foundation for support.

References

[1] G.E. Busch, R.T. Mahoney, R.I. Morse and K.R. Wilson, *J. Chem. Phys., 51* (1969) 449. G.E. Busch, J.F. Cornelius, R.T. Mahoney, R.I. Morse, D.M. Schlosser and K.R. Wilson, *Rev. Sci. Instrum., 41* (1970) 1066.

[2] R. Bersohn, *IEEE J. Quantum Electron., 16* (1980) 1208. S.R. Leone, *Adv. Chem. Phys., 50* (1982) 255. R. Bersohn, *J. Phys. Chem., 88* (1984) 5145. A.M. Wodtke and Y.T. Lee, in M.N.R. Ashfold and J.E. Baggott (eds.), *Molecular Photodissociation Dynamics*, Royal Socciety of Chemistry, London, 1987, p. 31.

[3] R.K. Sparks, L.R. Carlson, K. Shobatake, M.L. Kowalczyk and Y.T. Lee, *J. Chem. Phys., 72* (1980) 1401. A.M. Wodtke and Y.T. Lee, *J. Phys. Chem., 89* (1985) 4744. R.E. Continetti, B.A. Balko and Y.T. Lee, *J. Chem. Phys., 89* (1988) 3383.

[4] G.N.A. van Veen, K.A. Mohamed, T. Baller and A.E. de Vries, *Chem. Phys., 74* (1983) 261.

[5] Z. Xu, B. Koplitz and C. Wittig, *J. Chem. Phys., 90* (1989) 2692.

[6] H.J. Krautwald, L. Schnieder, K.H. Welge and M.N.R. Ashfold, *Faraday Discuss. Chem. Soc., 82* (1986) 99.

[7] C. Jonah, *J. Chem. Phys., 55* (1971) 1915.

[8] R.N. Zare, *Mol. Photochem., 4* (1972) 1.

[9] S. Yang and R. Bersohn, *J. Chem. Phys., 61* (1974) 4400.

[10] M. Dzvonik, S. Yang and R. Bersohn, *J. Chem. Phys., 61* (1974) 4408.

[11] S.R. Gandhi, T.J. Curtiss and R.B. Bernstein, *Phys. Rev. Lett., 59* (1987) 2951.

[12] S.M. Penn, C.C. Hayden, K.J. Carlson Muykens and F.F. Crim, *J. Chem. Phys., 89* (1988) 2909.

[13] J.F. Black and I. Powis, *Chem. Phys., 125* (1988) 375.

[14] T.A. Spiglanin and D.W. Chandler, *Chem. Phys. Lett., 141* (1987) 428.

[15] R. Ogorzalek Loo, G.E. Hall, H.-P. Haerri and P.L. Houston, *J. Phys. Chem., 92* (1988) 5. R. Ogorzalek Loo, H.-P. Haerri, G.E. Hall and P.L. Houston, *J. Chem. Phys., 90* (1989) 4222.

[16] M.P. Docker, A. Hodgson and J.P. Simons, in M.N.R. Ashfold and J.E. Baggott (eds.), *Molecular Photodissociation Dynamics*, Royal Society of Chemistry, London, 1987, p. 115. P.L. Houston, *J. Phys. Chem., 91* (1987) 5388.

[17] H.J. Hwang and M.A. El-Sayed, *J. Chem. Phys., 94* (1991) 4877.

[18] H.J. Hwang, *Doctoral Dissertation*, University of California, Los Angeles, CA, 1991. H.J. Hwang, J. Griffiths and M.A. El-Sayed, *Int. J. Mass Spectrom. Ion Processes, 131* (1994) 265.

[19] H.J. Hwang and M.A. El-Sayed, *J. Phys. Chem., 95* (1991) 8044.

[20] J.E. Freitas, H.J. Hwang, A.B. Ticknor and M.A. El-Sayed, *Chem. Phys. Lett., 183* (1991) 165.

[21] H.J. Hwang and M.A. El-Sayed, *J. Chem. Phys., 96* (1992) 856.

[22] H.J. Hwang and M.A. El-Sayed, *J. Phys. Chem., 96* (1992) 8728.

[23] J.E. Freitas, H.J. Hwang and M.A. El-Sayed, *J. Phys. Chem., 97* (1993) 12481; *J. Phys. Chem., 98* (1994) 3322; *J. Phys. Chem., 99* (1995) 7395.

[24] R.S. Mulliken, *J. Chem. Phys., 8* (1940) 382.

[25] S.J. Riley and K.R. Wilson, *Faraday Discuss. Chem. Soc., 53* (1972) 132.

[26] R.K. Sparks, K. Shobatake, L.R. Carlson and Y.T. Lee, *J. Chem. Phys., 75* (1981) 3838.

[27] G.N.A. van Veen, T. Baller, A.E. de Vries and N.J.A. van Veen, *Chem. Phys., 87* (1984) 405. G.N.A. van Veen, T. Baller, A.E. de Vries and M. Shapiro, *Chem. Phys., 93* (1985) 277.

[28] A. Gedanken and M.D. Rowe, *Chem. Phys. Lett., 34* (1975) 39. (b) A. Gedanken, *Chem. Phys. Lett., 137* (1987) 462.

[29] J.L. Knee, L.R. Khundkar and A.H. Zewail, *J. Chem. Phys., 83* (1985) 1996.

[30] M. Kawasaki, S.J. Lee and R. Bersohn, *J. Chem. Phys., 66* (1977) 2647. A. Freedman, S.C. Yang, M. Kawasaki and R. Bersohn, *J. Chem. Phys., 72* (1980) 1028.

[31] P.Y. Cheng, D. Zhong and A.H. Zewail, *Chem. Phys. Lett., 237* (1995) 399.

[32] D.F. McMillen and D.W. Golden, *Annu. Rev. Phys. Chem., 33* (1982) 493.

[33] S.W. Benson, *J. Chem. Educ., 42* (1965) 502.

[34] W.H. Pence, S.L. Baughcum and S.R. Leone, *J. Phys. Chem., 85* (1981) 3844.

[35] M.J. Rosker, M. Dantus and A.H. Zewail, *Science, 241* (1988) 1200. M. Dantus, M.J. Rosker and A.H. Zewail, *J. Chem. Phys., 89* (1988) 6128.

[36] R.A. Durie, T. Iredale and J.M.S. Jarvie, *J. Chem. Soc.*, (1950) 1181. T.M. Dunn and T. Iredale, *J. Chem. Soc.*, (1952) 1592.

[37] T. Pavlopoulos and M.A. El-Sayed, *J. Chem. Phys., 41* (1964) 1082. M.A. El-Sayed, *J. Chem. Phys., 43* (1965) 2864.

[38] M.A. El-Sayed, *Proc. Int. Conf. on Luminescence*, 1966 p. 373.